

Instability of two-dimensional graphene: Breaking sp^2 bonds with soft x rays

S. Y. Zhou,^{1,2} Ç. Ö. Girit,^{1,2} A. Scholl,³ C. J. Jozwiak,^{1,2} D. A. Siegel,^{1,2} P. Yu,¹ J. T. Robinson,^{2,4,*} F. Wang,¹ A. Zettl,^{1,2} and A. Lanzara^{1,2}

¹*Department of Physics, University of California, Berkeley, California 94720, USA*

²*Materials Sciences Division, Lawrence Berkeley National Laboratory, Berkeley, California 94720, USA*

³*Advanced Light Source, Lawrence Berkeley National Laboratory, Berkeley, California 94720, USA*

⁴*Department of Materials Science and Engineering, University of California, Berkeley, California 94720, USA*

(Received 8 July 2009; revised manuscript received 2 September 2009; published 29 September 2009)

We study the stability of various kinds of graphene samples under soft x-ray irradiation. Our results show that in single-layer exfoliated graphene (a closer analog to two-dimensional material), the in-plane carbon-carbon bonds are unstable under x-ray irradiation, resulting in nanocrystalline structures. As the interaction along the third dimension increases by increasing the number of graphene layers or through the interaction with the substrate (epitaxial graphene), the effect of x-ray irradiation decreases and eventually becomes negligible for graphite and epitaxial graphene. Our results demonstrate the importance of the interaction along the third dimension in stabilizing the long range in-plane carbon-carbon bonding, and suggest the possibility of using x-ray to pattern graphene nanostructures in exfoliated graphene.

DOI: [10.1103/PhysRevB.80.121409](https://doi.org/10.1103/PhysRevB.80.121409)

PACS number(s): 73.20.-r, 71.55.Ak, 73.21.Ac

The existence and stability of two-dimensional (2D) materials has been a fundamental yet long-debated subject. Graphene, a purely one-atom-thick two-dimensional material formed by carbon atoms arranged in a honeycomb lattice, was previously presumed not to exist because strictly two-dimensional materials are thermodynamically unstable.¹⁻³ The recent discovery of graphene^{4,5} has raised renewed interest regarding the long-debated issue about the stability of two-dimensional materials. Although it has been proposed recently that the ripples—corrugation along the third dimension in free-standing exfoliated graphene samples help to stabilize graphene,⁶⁻⁸ no direct experimental evidence about what causes the stability of the sp^2 bonds has been obtained so far. Here we present direct experimental proof that it is indeed the interaction along the third dimension that drives the stability of the graphene sheet. In particular we show that the closer the graphene sample is to a two-dimensional crystal, the easier it is for the sp^2 bonds to be broken under soft x-ray irradiation, resulting in nanocrystalline structures. This conclusion was based on a systematic study of various kinds of graphene samples with different amount of interaction along the third dimensionality, including exfoliated graphene on SiO_2 , suspended exfoliated graphene, and epitaxial graphene on SiC, and by combining two important techniques—x-ray absorption spectroscopy, which is sensitive to the sp^2 bonding, and Raman spectroscopy which is sensitive to the edges of the graphene samples.^{9,10} Our results show the direct evidence about the instability of two-dimensional graphene, and points out a possible route of using x-rays to engineer graphene nanoribbons.

The samples studied were exfoliated graphene samples on SiO_2/Si and epitaxial graphene on SiC. The thickness of exfoliated graphene samples is characterized by optical contrast^{11,12} and confirmed by Raman measurements.^{13,14} The thickness of epitaxial graphene is characterized by low-energy electron microscope (LEEM).¹⁵ Although the overall electronic structure of graphene is preserved in both types of graphene samples, the interaction along the third dimension is much stronger in epitaxial graphene than exfoliated

graphene. This is manifested by the formation of a first carbon rich layer strongly bonded with the SiC substrate,¹⁶ and the opening of a gap in the π bands for the first graphene layer.^{17,18} X-ray absorption spectroscopy (XAS) spectra at the C 1s edge were taken with photoemission electron microscope (PEEM) at PEEM2 of the Advanced Light Source (ALS) in Berkeley. The microscope is operated in the total electron yield (TEY) mode by recording the intensity maps while sweeping the photon energy across the C K edge. The photon flux was cut down to only 1/3 of the regular value to decrease the x-ray radiation damage on the sample. Raman spectra were taken on a commercial system (Renishaw inVia) at a wavelength of 514 nm (Argon laser). Special care was taken to minimize laser exposure on samples and subsequent spectra at the same spot showed no change. The spatial resolution of both techniques allows easy detection of each graphene region with different thickness.

Figure 1(a) shows the optical image of a typical exfoliated sample. Clear optical contrast can be observed between regions of graphene with different sample thickness.⁵ Figure 1(b) shows the PEEM image taken at 279 eV photon energy before the C 1s K edge on the same sample. Similar to the optical image [Fig. 1(a)], strong intensity contrasts between different regions are observed in the PEEM image shown in Fig. 1(b). Thicker graphene regions will appear darker in the pre-edge spectra because photoelectrons travel through more materials before being emitted to the vacuum, thus making PEEM another powerful tool to capture the thickness of graphene films. Figure 1(c) shows the C 1s XAS spectra taken on single-layer exfoliated graphene with two different polarizations. The two main features at ≈ 285 eV, and at ≈ 292 eV, correspond, respectively, to the π^* orbitals at the K and M points of the Brillouin zone and to the σ^* orbitals at the Γ point.¹⁹ Their in-plane and out-of-plane characters are confirmed by the dependence from the polarization of the incident photons [Fig. 1(c)].¹⁹ More specifically, when the light polarization is in-plane, only the in-plane σ^* orbital at 292 eV contributes to the C 1s edge, while when the out-of-

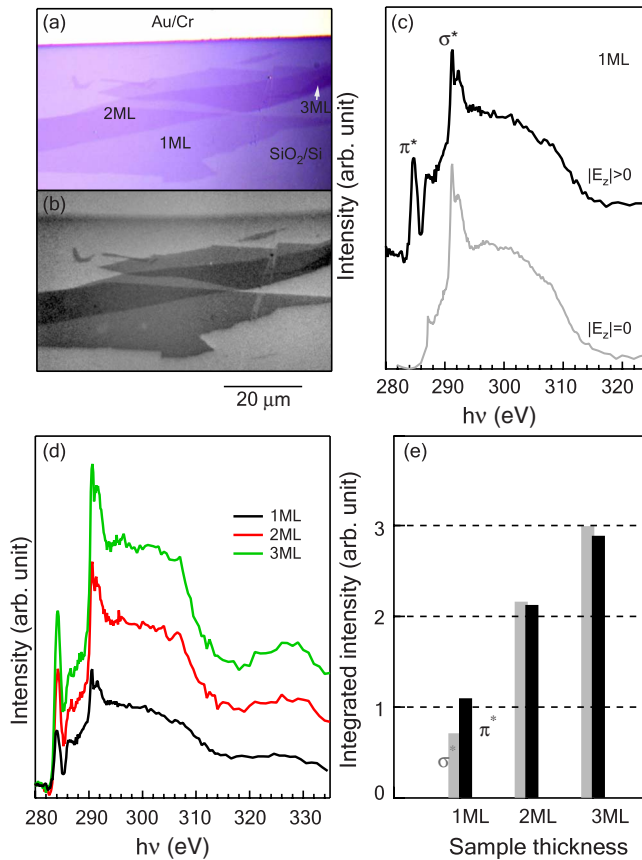


FIG. 1. (Color online) (a) Optical image of a representative exfoliated sample under study with different sample thickness. The electrical contact to the graphene samples is provided by a region of Au/Cr electrode (region on the top of panel a) deposited on the SiO₂. (b) PEEM image of the same sample taken at photon energy of 279 eV, just below the C 1s absorption edge. The spectra are normalized by the spectrum from Au on the same wafer. (c) C 1s spectra taken on single-layer exfoliated graphene with zero (gray curve) and nonzero (black curve) out-of-plane polarization components (E_z), respectively. (d) C 1s spectra taken from single-layer, bilayer, and trilayer graphene with nonzero out-of-plane polarization. (e) Area of the π^* and σ^* peaks as a function of the sample thickness extracted from data shown in panel d, after subtraction of a smooth background. The dotted lines are guides for the eyes.

plane polarization component increases, the intensity of the π^* feature at 285 eV strongly increases.

In Fig. 1(d) we show the C 1s spectra of exfoliated graphene for different sample thickness. As in Fig. 1(c), the π^* feature and the splitting of the σ^* orbitals are observed in all the spectra, independent of the sample thickness. The main difference is that as the thickness increases, the intensity of the σ^* and π^* features increases.

The high energy resolution and sample quality of this experiment has enabled us to clearly resolve the splitting of the σ^* peaks, not observed in a previous study,²⁰ and hence to quantify the thickness dependence of the absorption spectra and directly compare it to the optical reflectivity data. In Fig. 1(e) we show the integrated absorption intensity, determined from the area underneath the π^* and σ^* orbitals near the C K edge. The data clearly show that the intensity of the π^* and

the σ^* orbitals scales linearly with the sample thickness for up to three layers. Interestingly, this is in close analogy to the quantized steps observed in optical reflectivity and transmission for different graphene thickness,^{11,12} which are defined only by the fine-structure universal constant $\alpha = e^2/\hbar c$.¹² This result suggests that, even at higher photon energies the universality still holds and the absorption spectra is still related to the universal constant α , the parameter that defines the optical transparency of graphene.

Figure 2 shows the time evolution of the absorption spectra for exfoliated (panels a–d) and epitaxial (panel e) graphene. The relative intensity ratio of the σ^* to the π^* orbital show a clear time dependence from x-ray exposure. More specifically, the time dependence of the spectra is strongest for exfoliated single-layer graphene [Fig. 2(a)], as measured from the 24% change in the intensity ratio of the σ^* orbital to the π^* orbital, and decreases significantly as the number of layer increases, from 20% in bilayer to 15% in trilayer graphene. These findings suggest a strong radiation-induced damage of the exfoliated graphene upon soft x-ray exposure, a surprising result considering the inert character of carbon. This is reminiscent of the radiation-induced damage observed in carbon rich biological samples.²¹ We note that, although the radiation-induced damage presented here is observed for all the samples studied (more than five samples in total), in some cases the absorption spectra of single-layer graphene shows more dramatic changes. In an extreme case [inset in Fig. 2(a)], the signal of the σ^* orbital completely disappeared (pointed to by a gray arrow) and an additional peak arose before the adsorption edge (pointed to by a red arrow), reminiscent of the edge states observed in nanographite sample.²²

The strong radiation-induced change of the single-layer exfoliated graphene [Fig. 2(a)] is in contrast to the almost negligible effect observed on the epitaxial sample [Fig. 2(e)]. As for the exfoliated sample, the two main features in the spectra are the π^* and the σ^* orbitals, which occur at the same energy, a further confirmation that the overall electronic structure of exfoliated and epitaxial graphene is similar in nature. In this case however, the relative intensity of the π^* to the σ^* peak is much weaker, suggesting that the π^* derived states are partially occupied. This is likely due to a charge transfer from the buffer layer, in agreement with photoemission measurements reporting an highly doped nature of this sample.¹⁷ Note that, in addition to these main features, other peaks are observed above the σ^* peak, likely due to the substrate, as observed from a direct comparison with the absorption spectra of SiC.²³

The time dependence of the spectra in Fig. 2(e) clearly shows that the epitaxial sample is very stable and the damage induced by x-ray irradiation is negligible, despite the much longer exposure time. This result is in striking contrast with the strong time dependence observed in the exfoliated sample [Fig. 2(a)]. Note that these two types of samples were measured in the same chamber under the same conditions, and therefore this substantial difference in stability should be attributed to their intrinsic nature, e.g., the different strength of interaction along the third dimension, and not an artifact of the measurements.

To better understand the origin of this radiation-induced

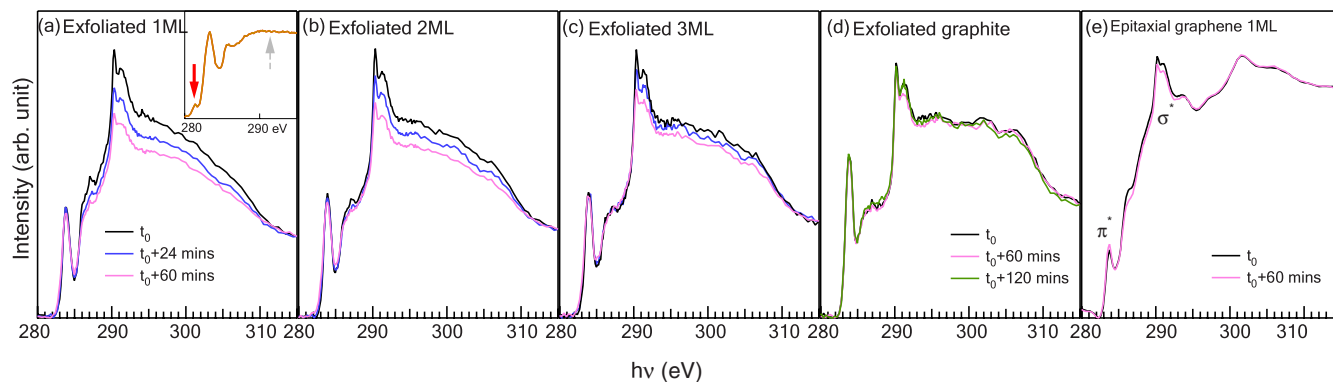


FIG. 2. (Color online) Time dependence of the C 1s XAS for (a) single-layer (b) bilayer, and (c) trilayer exfoliated graphene (d) exfoliated graphene and (e) epitaxial single-layer graphene. The spectra are offset to have zero intensity in the pre-edge and normalized to the same value at 315 eV for each sample. The inset in panel a shows an extreme sample which has negligible σ^* signal (pointed to by the gray arrow) after irradiation and additional pre-edge peak (pointed to by the red arrow) which is likely associated with edge states.

change, we compare Raman measurements on the same samples measured before and after exposure to soft x-rays (see Fig. 3). Before exposure, the exfoliated graphene sample shows a sharp G peak induced by the zone-center E_{2g} phonon at ≈ 1570 cm^{-1} , and a strong 2D peak (overtone of the zone-boundary A_{1g} phonon) at ≈ 2700 cm^{-1} . The 2D peak in single-layer graphene shows a single component, while the 2D peak for bilayer, trilayer graphene and many layer graphite is broader and contains multiple components, in agreement with previous studies.^{13,14} The sharpness of the G and 2D peaks, as well as the absence of the disorder-induced D peak at ≈ 1360 cm^{-1} ,^{9,10,24} D'' peak at ≈ 2950 cm^{-1} , shows that the samples under study are of very high quality, and the amount of disorder is negligible. However, after x-ray exposure, the Raman spectra show significant changes in all the

exfoliated samples, although the degree of change decreases from single-layer to trilayer graphene and almost disappear for graphite, in line with the absorption results previously discussed. More specifically, we observe the appearance of a huge D peak at 1360 cm^{-1} , as well as the appearance of D' peak at 1620 cm^{-1} and D'' peak at ≈ 2950 cm^{-1} . These changes are accompanied by the broadening of both the G (1570 cm^{-1}) and 2D (2700 cm^{-1}) peaks. In line with the absorption results (see Fig. 2), the comparison between graphene samples with different thickness suggests that the largest radiation-induced changes occur on the single-layer exfoliated graphene sample. On the contrary, the Raman spectrum for the single-layer epitaxial graphene shows negligible change, although it has been exposed to x-ray for a much longer time (≈ 10 h), once again pointing to the different nature between exfoliated and epitaxial graphene, and a better stability of the latter to x-ray irradiation.

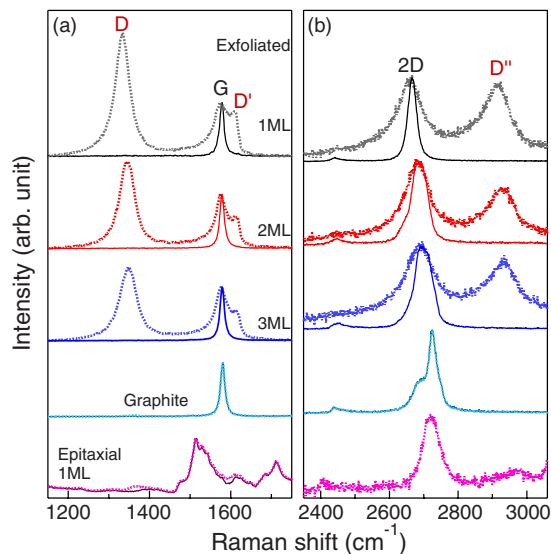


FIG. 3. (Color online) Raman spectra for exfoliated samples with different sample thickness (1, 2, and 3ML and graphite) and single-layer epitaxial graphene with laser excitation wavelength of 514 nm in the energy range near the D (a) and 2D peak (b). The solid and the dotted curves are taken before and after x-ray irradiation. The spectra are normalized to have the same amplitude for the G peak and 2D peak.

The results presented here point to a scenario where the x-rays locally break the sp^2 bonding giving rise to small crystallites within the same graphene sheet. This is supported by: (1) the decrease, or in some cases even the disappearance, in the σ^* -orbital-related signal in the absorption spectra (Fig. 2), suggesting a decrease in sp^2 bonded carbon atoms; (2) the appearance of a broad pre-edge feature [inset of Fig. 2(a)] in the absorption spectra, similar to that observed in nanographite edges;²² (3) the appearance of strong D, D' peaks in the Raman spectra (Fig. 3), associated with an increase of broken carbon bonds and edges states;^{9,10,14,24,25} and (4) the broadening of the G and 2D peak in the Raman spectra, suggestive of phonon confinement. The average crystallite size estimated from the ratio between the G and D peaks in the Raman spectra¹⁰ changes from 7 nm in single-layer exfoliated graphene to 10 and 12 nm in bilayer and trilayer exfoliated graphene, respectively, pointing to a smaller irradiation induced bond-breaking effect in thicker exfoliated graphene samples.

There are a few possibilities about the bond-breaking mechanism, and further investigation is needed to pin down the exact mechanism. First, the higher probability of bond breaking by x-rays in insulating samples²⁶ suggests that the bond breaking in graphene, which is a semimetal, might be caused by the ejection of electrons into the vacuum and the

insufficient restoration of the ejected electrons as a result of its low charge carrier concentration. This is particularly so considering that the SiO₂ layer underneath the graphene sample is quite insulating as well. Another possibility is that in exfoliated graphene, the SiO₂ substrate or even residual water between graphene and the SiO₂ layer might act as a “catalyst” for the sp² bond breaking through formation of epoxy groups or carbon mono-oxide groups. To test the second possibility, we have measured two bilayer graphene samples partially suspended on a few μm width trenches and we have detected a very similar amount of *D* peak in both the suspended and unsuspended regions after x-ray irradiation. This suggests that whatever the bond-breaking mechanism is, it must be intrinsic to the exfoliated graphene, and irrelevant of the SiO₂ substrates or the trapped water or gas between graphene and the SiO₂. As shown above, the radiation-induced bond-breaking effect also decreases when the interaction along the third dimension increases either by increasing the number of layers or through a stronger interaction with the substrate, suggesting the important role of the interaction along the third dimensionality.

In summary, we found that single-layer exfoliated

graphene is unstable under soft x-ray exposure, resulting in local breaking of the sp² bonding and the formation of small crystallites within the sample. As the interaction along the third dimension increases, either by increasing the sample thickness or through stronger bonding with the substrate, as in the case of epitaxial graphene, the graphene sample becomes more stable. These results point to the crucial role of the interaction along the third dimension in stabilizing quasi-two-dimensional graphene. Finally, this ability to easily break the carbon-carbon bonds suggests the possibility of using x-rays or even lasers²⁷ to “write” graphene nanostructures, an alternative to standard writing techniques. Further studies are needed to investigate where the bonds break²⁸ and to achieve a fine control of the amount of broken bonds.

We thank D.-H. Lee, A. K. Geim, and A. C. Ferrari for useful discussions. The photoemission and Raman measurements were supported by the Division of Materials Sciences and Engineering, Office of Basic Energy Sciences of the U.S. Department of Energy under Contract No. DE-AC03-76SF00098. A.Z. and C.O.G. acknowledge the DOE (Grant No. DE-AC02-05CH11231) for sample preparation and Raman characterization.

*Present address: Naval Research Laboratory, Washington, DC 20375.

¹N. D. Mermin and H. Wagner, *Phys. Rev. Lett.* **17**, 1133 (1966).

²N. D. Mermin, *Phys. Rev.* **176**, 250 (1968).

³L. D. Landau and E. M. Lifshitz, *Statistical Physics, Part I* (Pergamon, Oxford, 1980).

⁴K. S. Novoselov, A. K. Geim, S. V. Morozov, D. Jiang, Y. Zhang, S. V. Dubonos, I. V. Grigorieva, and A. A. Firsov, *Science* **306**, 666 (2004).

⁵K. S. Novoselov, D. Jiang, F. Schedin, T. J. Booth, V. V. Khotkevich, S. V. Morozov, and A. K. Geim, *Proc. Natl. Acad. Sci. U.S.A.* **102**, 10451 (2005).

⁶Jannik C. Meyer, A. K. Geim, M. I. Katsnelson, K. S. Novoselov, T. J. Booth, and S. Roth, *Nature (London)* **446**, 60 (2007).

⁷A. Fasolino, J. H. Jos, and M. I. Katsnelson, *Nature Mater.* **6**, 858 (2007).

⁸J. M. Carlsson, *Nature Mater.* **6**, 801 (2007).

⁹A. C. Ferrari, *Solid State Commun.* **143**, 47 (2007).

¹⁰M. A. Pimenta, G. Dresselhaus, M. S. Dresselhaus, L. G. Cançado, A. Jorio, and R. Saito, *Phys. Chem. Chem. Phys.* **9**, 1276 (2007).

¹¹Z. H. Ni, H. M. Wang, J. Kasim, H. M. Fan, T. Yu, Y. H. Wu, Y. P. Feng, and Z. X. Shen, *Nano Lett.* **7**, 2758 (2007).

¹²R. R. Nair, P. Blake, A. N. Grigorenko, K. S. Novoselov, T. J. Booth, T. Stauber, N. M. R. Peres, and A. K. Geim, *Science* **320**, 1308 (2008).

¹³A. C. Ferrari *et al.*, *Phys. Rev. Lett.* **97**, 187401 (2006).

¹⁴D. Graf, F. Molitor, K. Ensslin, C. Stampfer, A. Jungen, C. Hierold, and L. Wirtz, *Nano Lett.* **7**, 238 (2007).

¹⁵H. Hibino, H. Kageshima, F. Maeda, M. Nagase, Y. Kobayashi, and H. Yamaguchi, *Phys. Rev. B* **77**, 075413 (2008).

¹⁶Konstantin V. Emtsev, Thomas Seyller, F. Speck, Lothar Ley, P. Stojanov, J. D. Riley, and R. C. G. Leckey, *Mater. Sci. Forum* **556-557**, 525 (2007).

¹⁷S. Y. Zhou, G.-H. Gweon, A. V. Fedorov, P. N. First, W. A. de Heer, D.-H. Lee, F. Guinea, A. H. Castro Neto, and A. Lanzara, *Nature Mater.* **6**, 770 (2007).

¹⁸S. Kim, J. Ihm, H. J. Choi, and Y. W. Son, *Phys. Rev. Lett.* **100**, 176802 (2008).

¹⁹R. A. Rosenberg, P. J. Love, and V. Rehn, *Phys. Rev. B* **33**, 4034 (1986).

²⁰D. Pacile, M. Papagno, A. F. Rodriguez, M. Grioni, L. Papagno, C. O. Girit, J. C. Meyer, G. E. Begtrup, and A. Zettl, *Phys. Rev. Lett.* **101**, 066806 (2008).

²¹A. Kade *et al.*, *J. Phys. Chem. B* **111**, 13491 (2007).

²²Shiro Entani, Susumu Ikeda, Manabu Kiguchi, Koichiro Saiki, Genki Yoshikawa, Ikuyo Nakai, Hiroshi Kondoh, and Toshiaki Ohta, *Appl. Phys. Lett.* **88**, 153126 (2006).

²³M. Pedio *et al.*, *Phys. Scr.* **T115**, 308 (2005).

²⁴R. P. Vidano and D. B. Fischbach, *Solid State Commun.* **39**, 341 (1981).

²⁵A. C. Ferrari and J. Robertson, *Phys. Rev. B* **61**, 14095 (2000).

²⁶J. Cazaux, *J. Microsc.* **188**, 106 (1997).

²⁷A. Hu, M. Rybachuk, Q.-B. Lu, and W. W. Duley, *Appl. Phys. Lett.* **91**, 131906 (2007).

²⁸Çağlar Ö. Girit, Jannik C. Meyer, Rolf Erni, Marta D. Rossell, C. Kisielowski, Li Yang, Cheol-Hwan Park, M. F. Crommie, Marvin L. Cohen, Steven G. Louie, and A. Zettl, *Science* **323**, 1705 (2009).